Applied Physics Express **14**, 021004 (2021) **LETTER**
https://doi.org/10.35848/1882-0786/abdc9e

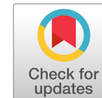

Influences of hydrogen ion irradiation on $N_CV_{Si}^-$ formation in 4H-silicon carbide

Takuma Narahara[1,2], Shin-ichiro Sato[2*], Kazutoshi Kojima[3], Yasuto Hijikata[1*], and Takeshi Ohshima[2]

[1]Graduate School of Science and Engineering, Saitama University, 255 Shimookubo, Sakura-ku, Saitama, Japan
[2]National Institutes for Quantum and Radiological Science and Technology (QST), 1233 Watanuki, Takasaki, Gunma, Japan
[3]National Institute of Advanced Industrial Science and Technology (AIST), Central 2, 1-1-1 Umezono, Tukuba, Ibaraki, Japan

*E-mail: sato.shinichiro2@qst.go.jp; yasuto@opt.ees.saitama-u.ac.jp

Received December 16, 2020; revised January 6, 2021; accepted January 15, 2021; published online January 28, 2021

Nitrogen-vacancy ($N_CV_{Si}^-$) center in 4H-SiC is spin defect with near-infrared luminescence at room temperature and a promising candidate for quantum technologies. This paper reports on $N_CV_{Si}^-$ center formation in N-doped 4H-SiCs by hydrogen ion irradiation and subsequent thermal annealing. It is revealed photoluminescence for $N_CV_{Si}^-$ centers suddenly appears above the fluence of 5.0×10^{15} cm^{-2} when annealed at 1000 °C. Appearance of a threshold fluence for their formation and/or activation has not been observed for other energetic particle irradiations. The possible mechanism is discussed based on the kinetics of hydrogen-related complexes and the majority carrier depletion caused by irradiation induced damage. © 2021 The Japan Society of Applied Physics

Spin defects in silicon carbide (SiC) are in high demand for quantum technologies such as quantum cryptography and quantum sensor applications.[1,2] Showing near-infrared (NIR) photon emissions at room temperature (RT), spin defects in SiC is particularly suitable for life-science applications such as in vivo imaging and sensing because of their high permeability in biological materials. Since large scale high-quality SiC wafers, matured SiC device fabrication technology and doping control are now available, integration of spin defects with SiC devices can potentially lead to realization of spin-based quantum hybrid devices.

For spin defects in SiC, single negatively charged silicon vacancy (V_{Si}^-)[2–5] and neutral divacancy ($V_{Si}V_C^0$)[6] have been studied and their high-fidelity spin state manipulation has been demonstrated. In addition to these spin defects, single negatively charged pair of V_{Si} and nitrogen atom (N) on an adjacent carbon (C) site ($N_CV_{Si}^-$ center) has recently shown as the promising spin defect since $N_CV_{Si}^-$ centers showed NIR photon emission around 1300 nm at RT.[7] This emission wavelength is longer than that of V_{Si}^- (900 nm) and $V_{Si}V_C^0$ (1100 nm), and thus the most suitable for quantum communication and quantum biosensing applications. Coherent control of $N_CV_{Si}^-$ center spins and optically detected magnetic resonance of single $N_CV_{Si}^-$ center at RT have been demonstrated.[8,9]

$N_CV_{Si}^-$ centers are formed by energetic particle irradiation and subsequent thermal annealing.[10] Hydrogen (H) ion beams (or proton beams) are generally used for the formation of optically active spin defects, since proton beam writing technique allows to control the defect-induced position three-dimensionally in sub-micron order.[3] Using this technology, optically active spin defects can be embedded with electric devices without deterioration. The effects on hydrogen irradiation fluence and subsequent thermal annealing need to be systematically clarified to control the formation of $N_CV_{Si}^-$ centers and to reduce undesired radiation induced defects. In this study, we reveal that the thermal annealing temperature exceeding 900 °C after H irradiation induces sudden drop on the $N_CV_{Si}^-$ center formation, despite the fact that in the case of heavy ion irradiations the highest photoluminescence (PL) intensity from $N_CV_{Si}^-$ centers has been obtained at around 1000 °C.[10] In addition, we show a threshold for the $N_CV_{Si}^-$ center formation on H irradiation fluence appears when annealed at 1000 °C. We discuss that these unique features of annealing temperature and irradiation fluence can be interpreted by a conflict with H-related complex defect formation.

Samples used in this study were intentionally nitrogen (N) doped 4H-SiC substrates with the concentration of $[N] = 9.0 \times 10^{18}$ cm^{-3} (4° off, Si-face) and N-doped 4H-SiC epilayers grown on the substrates ($[N] = 3.5 \times 10^{18}$ cm^{-3} and $[N] = 2.1 \times 10^{17}$ cm^{-3}). The samples were irradiated with 240 keV-H ions ranging from 1.0×10^{15} cm^{-2} to 5.0×10^{16} cm^{-2} at RT at the Takasaki Advanced Radiation Research Institute, National Institutes for Quantum and Radiological Science and Technology. The depth of peak defect concentrations from the sample surface was estimated to be 1.5 μm, according to the Monte Carlo Simulation Code, TRIM.[11] The samples were thermally annealed after irradiation under Ar atmosphere (1 atom) for 30 min. The annealing temperature ranged from 800 °C to 1100 °C. PL properties at the irradiated region in the samples at 80 and 293 K (RT) were investigated using HORIBA LabRAM HR Evolution (micro-PL measurement system). The excitation laser wavelength was 1064 nm and PL ranging from 1100 to 1600 nm from the samples was collected with an objective lens (numerical aperture, NA is 0.50 at 80 K and 0.90 at RT) and detected by an InGaAs array detector. The estimated laser spot diameter and the net laser power were 2.6 μm and 74.8 mW at 80 K, and 1.4 μm and 161 mW at 293 K, respectively. Only the photon emission from the irradiated region was collected in this study since the ideal axial resolution of the measurement system was estimated to be 5 μm when the refractive index of SiC was 2.6.[12]

Figure 1 shows NIR-PL spectra of the sample at 80 K and RT. Three peaks appeared at 1128.0 nm, 1160.6 nm, and 1186.5 nm in the as-grown sample (black lines) are assigned to the Raman shift of nitrogen donors, E_2 planar optical and A_1 longitudinal optical phonons, respectively.[10,13] A broad peak appeared at 1200 nm after irradiation of 240 keV-H ions at the fluence of 1.0×10^{16} cm^{-2} (red lines) is thought to be related to vibrational modes from the significantly deteriorated lattice structures. It has been reported that two broad peaks at 200–400 cm^{-1} (1087–1111 nm) and 400–600 cm^{-1} (1111–1134 nm) due to Si–Si vibration modes, one broad peak at 600–1000 cm^{-1} (1137–1191 nm) due to Si–C vibration modes, and two broad peaks at 1000–1200 cm^{-1} (1091–1220 nm) and 1200–1600 cm^{-1} (1220–1282 nm) due to C–C vibration modes

 © 2021 The Japan Society of Applied Physics

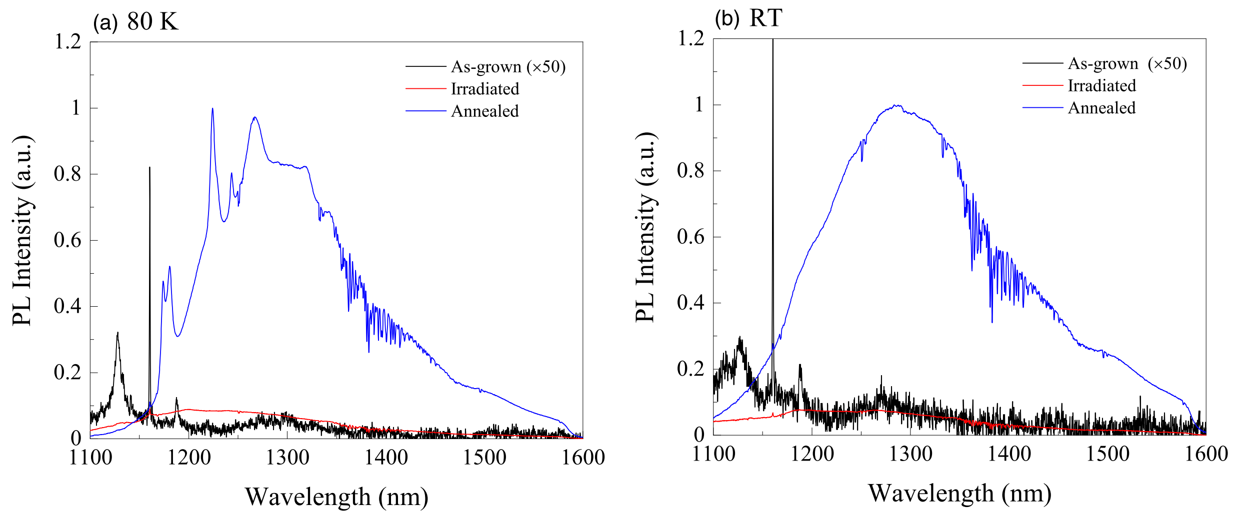

Fig. 1. (Color online) NIR-PL spectra of the [N] = 9.0×10^{18} cm^{-3} sample at (a): 80 K and (b): RT excited by 1064 nm. Black, red, blue lines show the PL spectra for as-grown, as-irradiated with 240 keV-H at the fluence of 1.0×10^{16} cm^{-2}, and after thermal annealing at 1000 °C for 30 min in Ar atmosphere, respectively. The PL spectra of as-grown samples (black lines) are scaled by a factor of 50.

appeared after ion irradiation.[14] Convolution of these vibrational modes yield the broad PL spectra centered around 1200 nm. After thermal annealing at 1000 °C, four sharp peaks at 1173.7 nm, 1179.7 nm, 1223.7 nm, and 1243.8 nm appeared at 80 K and a broad PL spectrum in the range of 1100–1600 nm also appeared at RT (blue lines). These four peaks and the broad peak were attributed to $N_CV_{Si}^-$ zero-phonon lines and their phonon-sidebands. These features were in good agreement with the previous reports.[7] Note that the fringe appeared at 1350–1450 nm is due to the absorption of water in the air.

Figure 2 shows variation of the $N_CV_{Si}^-$ PL intensity as a function of 240 keV-H ion fluence at RT. The ordinate is the PL intensity integrated from 1150 to 1450 nm. In the case of the [N] = 9.0×10^{18} cm^{-3} samples after annealing at 900 °C, the PL intensity increased with increasing fluence up to 5.0×10^{15} cm^{-2} and then slightly decreased. In the case of 1000 °C annealing, however, no significant PL from $N_CV_{Si}^-$ centers appeared below 5.0×10^{15} cm^{-2} (low fluence regime), the PL intensity drastically increased above 5.0×10^{15} cm^{-2} (threshold regime) and saturated or slightly decreased above 1.0×10^{16} cm^{-2} (high fluence regime). The same trend was also obtained from the results of the other samples ([N] = 3.5×10^{18} cm^{-3} and 2.1×10^{17} cm^{-3}), although appearance of the threshold fluence has not been found for other ion species (nitrogen, silicon, and iodine ion beams).[14] We further investigated the dependence of 380 keV-helium (He), 50 MeV-He and 200 MeV-neon (Ne) ion fluence for comparison to the results of 240 keV-H. Thermal annealing at 1000 °C was performed after irradiation. The results are shown in Fig. 2(b). The vacancy concentration profiles for their ion beams, calculated by TRIM, are also shown in Fig. 2(c). Note that the PL intensity at the Bragg peak region was characterized for 380 keV-He and 200 MeV-Ne, while the surface region was characterized for 50 MeV-He as the ion range was far longer than the sample thickness. The results showed that the PL integrated intensity monotonically increased with increasing fluence and no threshold fluence was observed. Therefore, we conclude that the appearance of the threshold fluence after 1000 °C annealing is a unique phenomenon on H ion irradiation.

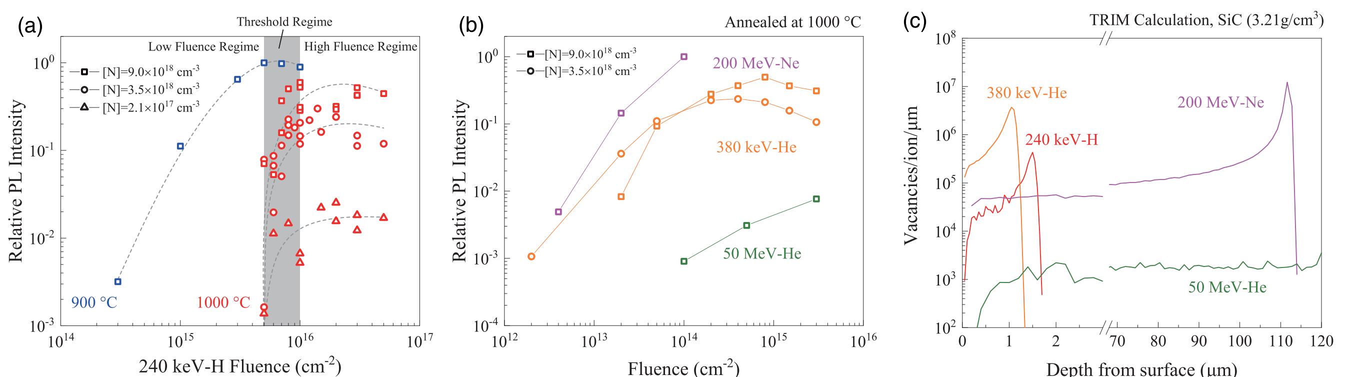

Fig. 2. (Color online) (a) PL integrated intensity of $N_CV_{Si}^-$ centers at RT as a function of 240 keV-H irradiation fluence. Open squares, circles, and triangles denote the results of [N] = 9.0×10^{18} cm^{-3}, 3.5×10^{18} cm^{-3}, and 2.1×10^{17} cm^{-3} samples, respectively. Dashed gray lines are drawn to guide the eye. No significant PL from $N_CV_{Si}^-$ centers was found at the fluence less than 5×10^{15} cm^{-2} (low fluence regime) when the annealing temperature was 1000 °C. (b) Results of 380 keV-He, 50 MeV-He, and 200 MeV-Ne irradiations at the annealing temperature of 1000 °C. The ordinate in (a) and (b) is the PL integrated intensity ranging from 1150 to 1450 nm. (c) Vacancy concentration profiles in SiC (3.21 g cm^{-3}) induced by ion beams used in this study, calculated by TRIM [11]. Lines in red, orange, purple, and green denote 240 keV-H, 380 keV-He, 200 MeV-Ne, and 50 MeV-He, respectively.

© 2021 The Japan Society of Applied Physics

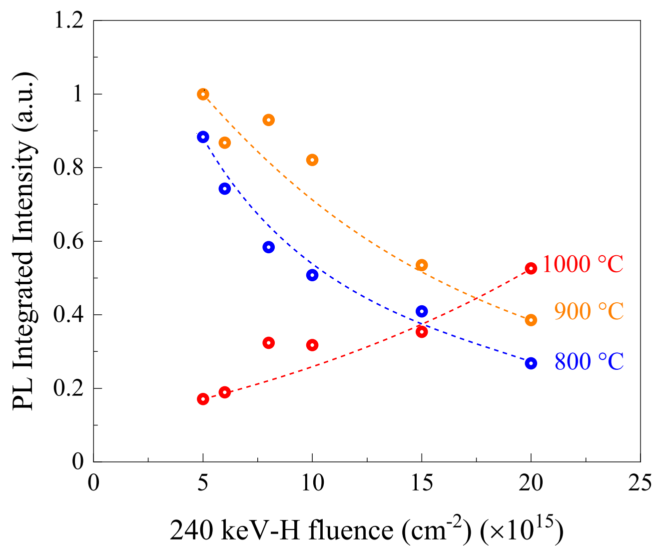

Fig. 3. (Color online) PL integrated intensity of the $[N] = 3.5 \times 10^{18}$ cm^{-3} samples at different thermal annealing temperatures (blue: 800 °C, orange: 900 °C, and red: 1000 °C). The ordinate is normalized by the value of 900 °C at 5.0×10^{15} cm^{-2}. Dashed lines are drawn to guide the eye.

Figure 3 shows the PL integrated intensity of the $[N] = 3.5 \times 10^{18}$ cm^{-3} samples as a function of fluence with different annealing temperatures. The PL from $N_CV_{Si}^-$ centers after annealing at 1000 °C increased with increasing fluence, being reduced at 800 °C and 900 °C. Since the thermal annealing at 900 °C is not high enough to sufficiently recover the crystallinity in the high fluence regime and radiation induced damage accumulates with increasing fluence even after annealing, the residual damage quenches the PL from $N_CV_{Si}^-$ centers. However, the highest PL intensity was found at 900 °C and it was reduced after annealing at 1000 °C when the irradiation fluence was below 1.5×10^{16} cm^{-2}. Moreover, no significant PL from $N_CV_{Si}^-$ centers appeared after annealing at 1100 °C. This trend is different from the annealing behavior for the other ion species. Previous studies have reported that the highest PL intensity was obtained at 1000°C–1050°C for the other ion species.[8,10]

Here, we discuss why the highest PL intensity from $N_CV_{Si}^-$ centers was obtained at thermal annealing of 900 °C while no significant PL from $N_CV_{Si}^-$ centers was observed after 1000 °C annealing at the low fluence regime. The discrepancy in annealing behavior for the other ions species suggests that in the case of H irradiation, different defect kinetics are involved with the $N_CV_{Si}^-$ center formation. This behavior can be attributed to quenching or deactivation of $N_CV_{Si}^-$ centers by H-related complex defect formation. It has been suggested from DLTS and PL analysis that in the case of n^+-type SiC, V_{Si}–H complex defects were mainly formed by thermal annealing above 400 °C and were stable up to 900 °C.[15,16] In contrast, $N_CV_{Si}^-$ centers are formed at temperatures above 700 °C.[10,17] Considering that V_{Si}–H complex defects are formed at lower annealing temperatures than $N_CV_{Si}^-$ centers (700 °C), both V_{Si}–H complex defects and $N_CV_{Si}^-$ centers are present at 700 °C–900 °C and defect reaction between them is likely to occur above 900 °C, resulting in the formation of other complex defects like N_CV_{Si}–H[18] and N_C–H.[19,20] N_C–H complex is known to be present even at 1700 °C. It has been reported that NVH complex defects quenched NV^- center emission in diamond.[21] Therefore, the formation of N_CV_{Si}–H and N_C–H complex defects in SiC is thought to be the cause of quenching of $N_CV_{Si}^-$ centers at the low fluence regime.

Unlike the case of low fluence regime, PL from $N_CV_{Si}^-$ centers appeared after 1000 °C annealing at the threshold and high fluence regime. This is thought to be caused by the change in charge state of embedded hydrogens. According to theoretical calculations,[15,19,22] H interstitial has the charge state of −1 (H_i^-) in n^+-type ($[N_D] = 10^{17}$– 10^{19} cm^{-3}) SiC and binds to other defects (e.g. V_{Si}) or ionized donors to be stable. On the other hand, in the case of weak n-type or p-type SiC, the stable charge state of H is neutral or +1 (H_i^0 or H_i^+) and they are not combined with other defects above RT.[23] It is likely that at the low fluence regime, H_i^- interstitials were combined with other defects and these defects quenched $N_CV_{Si}^-$ centers after thermal annealing at 1000 °C. The similar phenomenon has been observed for V_{Si}^- emissions in this fluence regime.[15]

The rapid increase in PL intensity at the threshold regime is thought to be caused by the change in charged state of implanted H atoms due to the carrier removal effect. In general, accumulation of defects by ion irradiation induces the decrease in effective donor concentration ($N_{D\phi}$) and the lowering of the Fermi level. The carrier removal effect generally follows the equation of $N_{D\phi} = N_{D0} \exp\left(\frac{-R_C\phi}{N_{D0}}\right)$, where N_D, R_C, and ϕ are the donor concentration, the carrier removal rate, and the irradiation fluence, respectively.[24,25] The subscripts "0" and "ϕ" refer to "before (initial)" and "after" irradiations, respectively. The initial donors ($[N_{D0}] = 3.5 \times 10^{18}$ cm^{-3}, for instance) were estimated to be almost depleted by the irradiation above 5.0×10^{15} cm^{-2} (threshold regime) when the R_C value of 2.0×10^4 cm^{-1} was used.[26] This indicates that at the high fluence regime, implanted H atoms are easily desorbed from the surface after thermal annealing since they have the charge state of 0 or +1 and do not bind to other defects. Thus, $N_CV_{Si}^-$ centers are never quenched at the high fluence regime due to the absence of V_{Si}–H complex defects. The saturation or reduction of PL intensity at the high fluence regime shown in Fig. 2 can be explained in terms of the amorphization. Significantly degraded SiC lattice structure by H irradiation does not fully recover even after thermal annealing at 1000 °C and the $N_CV_{Si}^-$ center formation is prevented.[14]

In summary, we investigated the $N_CV_{Si}^-$ center formation in 4H-SiCs by H-irradiation and annealing, and the dependence of irradiation fluence and thermal annealing temperature was clarified. We showed the threshold fluence at 5.0×10^{15} cm^{-2} for the $N_CV_{Si}^-$ center formation appeared at 1000 °C annealing. Below the threshold fluence, V_{Si}–H complex defects are formed and $N_CV_{Si}^-$ centers are quenched by the reaction with V_{Si}–H complexes. Above the threshold fluence, however, H interstitials are desorbed due to change in its dominant charge state and $N_CV_{Si}^-$ centers are formed. No threshold fluence appears when annealed at 900 °C, since the reaction between V_{Si}–H and $N_CV_{Si}^-$ can occur above 900 °C. This unique phenomenon has not been found for other ion species and this fact suggests that systematic understanding of the kinetics of implanted H atoms and the suppression of their complex defects is required to increase the creation yield of the $N_CV_{Si}^-$ center.

© 2021 The Japan Society of Applied Physics

Acknowledgments This study was supported by the QST President's Strategic Grant "Creative Research", the IAEA CRP F11020 and the JSPS KAKENHI Grant Numbers 17H01056, 18H03770 and 20H00355.

ORCID iDs Takuma Narahara https://orcid.org/0000-0002-5157-2442 Shin-ichiro Sato https://orcid.org/0000-0001-9359-9400 Yasuto Hijikata https://orcid.org/0000-0002-6314-0401 Takeshi Ohshima https://orcid.org/0000-0002-7850-3164

1) J. R. Weber, W. F. Koehl, J. B. Varley, A. Janotti, B. B. Buckley, C. G. V. de Walle, and D. D. Awschalom, Proc. Natl. Acad. Sci. U.S.A. **107**, 8513 (2010).
2) D. Riedel, F. Fuchs, H. Kraus, S. Väth, A. Sperlich, V. Dyakonov, A. A. Soltamova, P. G. Baranov, V. A. Ilyin, and G. V. Astakhov, Phys. Rev. Lett. **109**, 226402 (2012).
3) H. Kraus et al., Nano Lett. **17**, 2865 (2017).
4) T. Ohshima, T. Satoh, H. Kraus, G. V. Astakhov, V. Dyakonov, and P. G. Baranov, J. Phys. D **51**, 333002 (2018).
5) Y. Yamazaki, Y. Chiba, T. Makino, S.-I. Sato, N. Yamada, T. Satoh, Y. Hijikata, K. Kojima, S.-Y. Lee, and T. Ohshima, J. Mater. Res. **33**, 3355 (2018).
6) G. Wolfowicz, C. P. Anderson, A. L. Yeats, S. J. Whiteley, J. Niklas, O. G. Poluektov, F. J. Heremans, and D. D. Awschalom, Nat. Commun. **8**, 1876 (2017).
7) H. J. von Bardeleben, J. L. Cantin, A. Csóré, A. Gali, E. Rauls, and U. Gerstmann, Phys. Rev. B **94**, 121202 (2016).
8) Z. Mu et al., Nano Lett. **20**, 6142 (2020).
9) J. F. Wang et al., Phys. Rev. Lett. **124**, 223601 (2020).
10) S.-I. Sato, T. Narahara, Y. Abe, Y. Hijikata, T. Umeda, and T. Ohshima, J. Appl. Phys. **126**, 083105 (2019).
11) J. F. Ziegler, M. D. Ziegler, and J. P. Biersack, Nucl. Instrum. Methods B **268**, 1818 (2010).
12) S. Wang, M. Zhan, G. Wang, H. Xuan, W. Zhang, C. Liu, C. Xu, Y. Liu, Z. Wei, and X. Chen, Laser Photon. Rev. **7**, 831 (2013).
13) J. C. Burton, F. H. Long, and I. T. Ferguson, J. Appl. Phys. **86**, 2073 (1999).
14) T. Narahara, S.-I. Sato, K. Kojima, Y. Yamazaki, Y. Hijikata, and T. Ohshima, Mater. Sci. Forum **1004**, 349 (2020).
15) M. E. Bathen, A. Galeckas, J. Coutinho, and L. Vines, J. Appl. Phys. **127**, 085701 (2020).
16) G. Alfieri, E. V. Monakhov, and B. G. Svensson, J. Appl. Phys. **98**, 113524 (2005).
17) U. Gerstmann, E. Rauls, T. Frauenheim, and H. Overhof, Phys. Rev. B **67**, 205202 (2003).
18) P. Deák, B. Aradi, M. Kaviani, T. Frauenheim, and A. Gali, Phys. Rev. B **89**, 075203 (2014).
19) A. Gali, P. Deák, N. T. Son, and E. Janzén, Phys. Rev. B **71**, 035213 (2005).
20) F. Gendron, L. M. Porter, C. Porte, and E. Bringuier, Appl. Phys. Lett. **67**, 1253 (1995).
21) S. Chakravarthi, C. Moore, A. Opsvig, C. Pederson, E. Hunt, A. Ivanov, I. Christen, S. Dunham, and K.-M. C. Fu, Phys. Rev. Mater. **4**, 023402 (2020).
22) A. Barcz, M. Kozubal, R. Jakieła, J. Ratajczak, J. Dyczewski, K. Gołaszewska, T. Wojciechowski, and G. K. Celler, J. Appl. Phys. **115**, 223710 (2014).
23) B. Aradi, P. Deák, A. Gali, N. T. Son, and E. Janzén, Phys. Rev. B **69**, 233202 (2004).
24) S.-I. Sato, T. Ohshima, and M. Imaizumi, J. Appl. Phys. **105**, 044504 (2009).
25) A. A. Lebedev, V. V. Kozlovski, N. B. Strokan, D. V. Davydov, A. M. Ivanov, A. M. Strel'chuk, and R. Yakimova, Semiconductors **36**, 1270 (2002).
26) R. K. Nadella and M. A. Capano, Appl. Phys. Lett. **70**, 886 (1997).

 © 2021 The Japan Society of Applied Physics